

Short Communication

Do abrupt cryosphere events in High Mountain Asia indicate earlier tipping point than expected ?

Cun-De XIAO^a, Tong ZHANG^a, Tao CHE^b, Zhi-Qiang WEI^c, Tong-Hua WU^b, Lei HUANG^d, Ming-Hu DING^e, Qiao LIU^f, Dong-Hui SHANGGUAN^b, Fei-Teng WANG^b, Peng-Lin WANG^d, Jie CHEN^b, Chun-Hai XU^b, Xin-Wu XU^d, Da-He QIN^{b,*}

^a State Key Laboratory of Earth Surface Processes and Resource Ecology, Beijing Normal University, Beijing 100875, China

^b State Key Laboratory of Cryospheric Science, Chinese Academy of Sciences, Lanzhou 730000, China

^c Faculty of Arts and Sciences, Beijing Normal University, Zhuhai 519000, China

^d National Climate Center, China Meteorological Administration, Beijing 100081, China

^e Global Change and Polar Institute, Chinese Academy of Meteorological Science, Beijing 100081, China

^f Institute of Mountain Hazards and Environment, Chinese Academy of Sciences, Chengdu 610299, China

Received 7 December 2022; revised 6 October 2023; accepted 23 November 2023

Abstract

Tipping points of about 16 elements have been identified in Earth system, yet cryospheric tipping point of specific Alpine region has not been studied. Here we analyzed three tipping elements (mountain glacier, snow cover, and permafrost) identified in recent years, evidenced by the facts of frequent occurrence of abrupt massive collapse of glacier mass and the widespread thermakarst of permafrost. Since 2015, strikingly abrupt cryosphere events (ACEs) have been consistently observed over a large range of High Mountain Asia (HMA). Those events were unprecedentedly significant in history, leading to collapses of glaciers following by disconnection of glacier tongue from accumulation basin and recession of thermakarst towards higher elevation. Strong decreasing of snow depth in 2022 was also observed since 2021/2022 winter, coinciding with extreme warming of the year. The widespread high warming rates in the last two decades over HMA might have triggered above ACEs. The dynamic thresholds of ACEs depend largely on high temperature, especially extreme heat wave, for both glaciers and permafrost, closely related to meltwater as a key factor for reaching initial conditions of abrupt changes, suggesting HMA cryosphere is a tipping element under the global warming level of 1.1 °C. The ACEs can cause tremendous damage to local ecosystem and socioeconomy, measures to mitigate risks should be taken when the tipping points are reached.

Keywords: Abrupt glacier change; Thermakarst; Snow depth; Tipping point; Early warning system

1. Introduction

Human activities are accelerating changes in the Earth system at a scale and pace that is pushing the planet out of a safe operating space for humanity. These rapid changes

undermine all life-support systems, with significant impacts on society, and could trigger tipping points irreversibly and thus destabilize the Earth system. Tipping elements are those components or processes that regulate the function and state of the planet to maintain a stable Holocene-like climate, and that show evidence of having thresholds at which small additional perturbations can undermine Earth system stability and resilience.

McKay et al. (2022) synthesizes the latest evidences of how much climate warming would risk by passing 16 climate

* Corresponding author.

E-mail address: qdh@cma.gov.cn (QIN D.-H.).

Peer review under responsibility of National Climate Center (China Meteorological Administration).

<https://doi.org/10.1016/j.accre.2023.11.006>

1674-9278/© 2023 The Authors. Publishing services by Elsevier B.V. on behalf of KeAi Communications Co. Ltd. This is an open access article under the CC BY-NC-ND license (<http://creativecommons.org/licenses/by-nc-nd/4.0/>).

tipping points (CTPs). They identify nine global ‘core’ tipping elements which contribute substantially to Earth system functioning and seven regional ‘impact’ tipping elements which contribute substantially to human welfare or have great value as unique features of the Earth system. Current global warming of ~ 1.1 °C above pre-industrial level already lies within the lower end of five CTPs’ uncertainty ranges. Here we present evidences that cryosphere over high mountain Asia (HMA) is likely reaching tipping points with particular striking events of glacier collapse and large-scale thermokarst over permafrost region. For example, a recent expedition to Mt. Qomolangma (Everest) showed that the melt of glacier ice at a high elevation (above 6500 m a.s.l.) is accelerating, and snow depth displayed strong anomaly in 2022.

HMA is a high-elevation geographic region in Asia that includes numerous cordillera and highland systems around the Qinghai–Tibet Plateau, encompassing regions of East, Southeast, Central and South Asia. HMA was orogenically formed by the continental collision of the Indian Plate into (and underneath) the Eurasian Plate. HMA is largely covered by cryospheric components such as mountain glaciers, permafrost and snow cover, and it has the largest snow and ice reserves outside of the Greenland and Antarctica ice sheets. According to the Randolph Glacier Inventory (RGI), there are around 90,000 glaciers in the HMA (Pfeffer et al., 2014). The permafrost area approximates to 1.6 million km² in the HMA region (Obu et al., 2019). The HMA mountains supply fresh water into major river basins that support about 1.5 billion people for drinking water, irrigation, and hydropower. In this study, by analyzing the typical abrupt cryosphere events in HMA, we want to point out that the fragile cryosphere system changes in HMA may be approaching its dynamical tipping point from a stable state to a critical transition.

2. Emerging abrupt cryosphere events (ACEs) in HMA

At present, the HMA glaciers are generally suffered and dominated by negative mass balances (Brun et al., 2017). A range of natural and anthropogenic factors and processes modulate surface climate-induced glacier melt and retreat, resulting in widespread glacier shrinkage. Ice cores over HMA provide temperature changes in the last 2000 years (Yao et al., 2019), integrating four curves of air temperature into one curve (Fig. 1). The four ice cores, Guliya, Dunde, Puruogangri, and Dasuopu, were retrieved from west, east, middle, and south of the Qinghai–Tibet Plateau, respectively. Clearly, the warming rate after the 20th century is unprecedentedly high in the whole 2000 years (Chen et al., 2015).

Here, we show several important abrupt cryosphere events (ACEs) since 2015 that indicate clearly the signs of tipping point in HMA.

2.1. Striking HMA glacier ACEs in recent years

Collapse of mountain glaciers (e.g., Gilbert et al., 2018; Käab et al., 2018) is an extreme process enhancing glacier response to climatic forcing (IPCC, 2021). An improved

understanding and quantification of the impacts raised by these processes lead to a conclusion that a changing climate is the main driver of observed HMA regional glacier retreats. Over the past few decades, ice avalanches in HMA have generally increased, especially during 2000–2019 (Fig. 1b), with the frequency of avalanche events showing an accelerating trend (Acharya et al., 2023; Zhang et al., 2023). The majority of these avalanche events occur in the central and eastern regions of Himalayan mountain range, the Nyainqentanglha Mountains, and the Trans-Himalayan region. This may be related to the development of glacial lakes and maritime glaciers in these areas, making glaciers more prone to dynamic instability and abrupt changes. There are several striking events since 2015 as follows.

2.1.1. The 2015 Karayaylak Glacier collapse, Kongur Tagh, eastern Pamir

The Karayaylak Glacier is situated on the northern side of Kongur Tagh, eastern Pamir. According to the second Chinese glacier inventory, it is the largest glacier in east Pamir with an area of 115.2 km². The Karayaylak Glacier surged and collapsed in 2015, which submerged the surrounding meadows and houses (Shangguan et al., 2016). The mean surface velocity for the western tributary of the Karayaylak Glacier increased insignificantly from May to June 2014 (Peng et al., 2021). Other studies also indicated that glacier velocity increased markedly after May 2014 and a general low-value state ($0.26\text{--}0.47$ m d⁻¹) was observed from April 2013 to May 2014 (Zhang et al., 2022). The velocity continued to accelerate and reached a peak value (4.1 ± 0.8 m d⁻¹) during 11 April to 17 May 2015. During this period, ice crevasses, ice cliffs and ice fissures rapidly expanded at the high elevations of the western tributary, and the glacier tongue rapidly thickened and formed compressed glacial landforms. The surging area began to decelerate after July 2015 and surface velocity presented annual periodicity during 2017–2021 with the value ($0.6\text{--}1$ m d⁻¹) remaining slightly higher than those during the post-surge period (2015–2016).

Slightly thinning for Karayaylak Glacier was observed during the period 2000–2012 and we cannot clearly identify the reservoir and receiving zone (Zhang et al., 2022). The western tributary of the glacier experienced slightly thickening in the reservoir zone and thinning in the receiving zone during the second period 2012–2014, indicating that glacier mass migration expressed by surface elevation change signals the onset of the surge. In the third period 2014–2015, the mean surface elevation reduced by 33.1 ± 1.5 m in the reservoir zone and increased by 36.8 ± 1.5 m in the receiving zone, and the glacier mass loss in the reservoir zone is 15.2%–19.3% of the total glacier mass. In addition, glacier surface mass balance in 2015 is around -1859 mm w.e. based on *in-situ* glaciological measurements and the degree-day model, the change in mass caused by the glacier surge is 15.4×10^6 m³, which has caused the glacier ablation to increase by about 15% (Li, 2017).

The emerging of this abrupt glacier event can be attributed to climate warming, which increases warm ice regions and

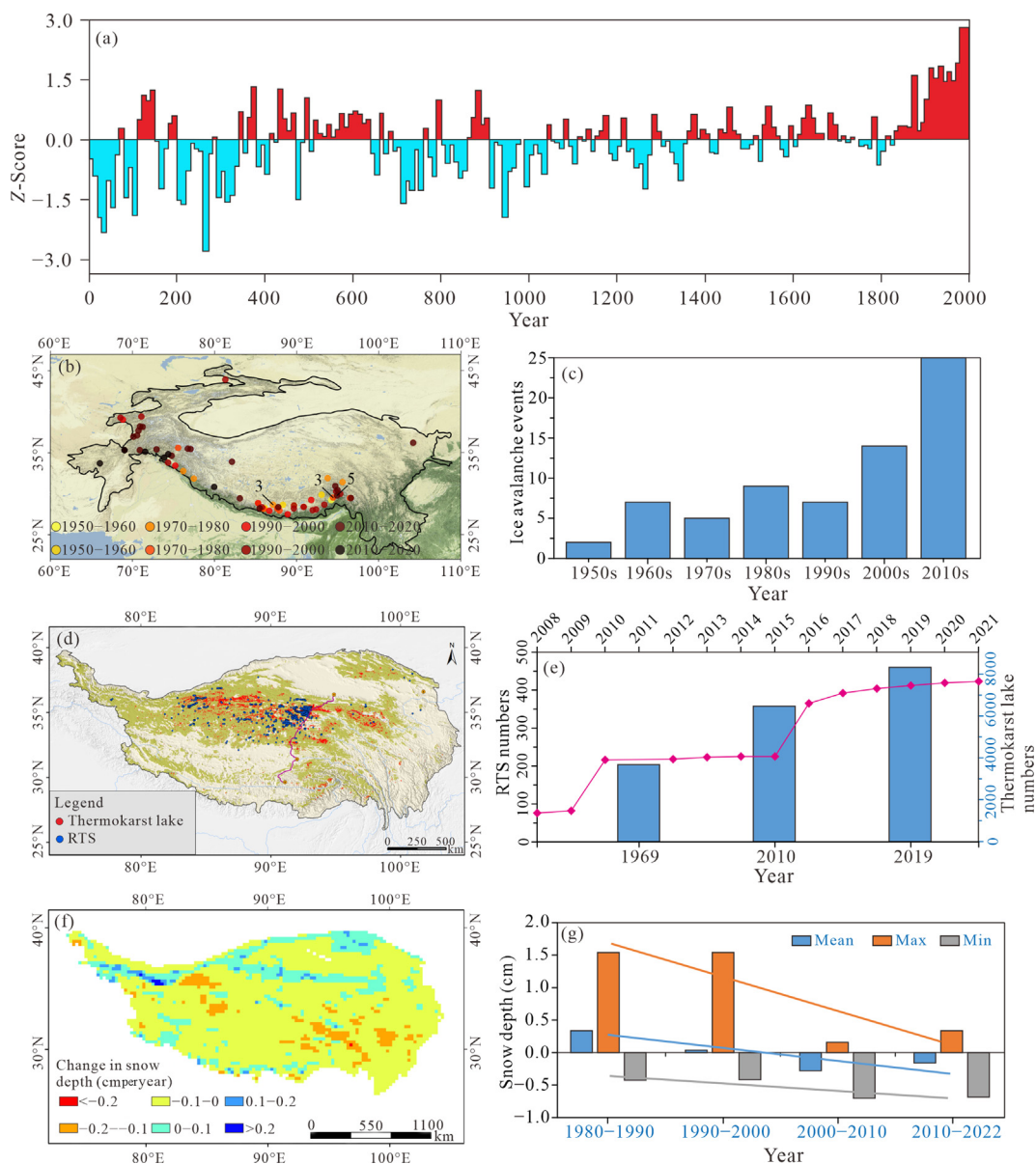


Fig. 1. Abrupt changes of main cryospheric components over HMA, (a) air temperature changes in the last 2000 years, by integrating four curves of air temperature recorded in four ice cores into one curve (Yao et al., 2019), with the Y-axis converted into Z-scores, (b–c) the distribution of ice collapse events occurred from the 1950s (1950–1959) to the 2010s (2010–2019) (Acharya et al., 2023; Zhang et al., 2023), (d–e) the distribution and changes of thermokarst landform on the Qinghai–Tibet Plateau (QTP), including thermokarst lake (Wei et al., 2021) and retrogressive thaw slump (RTS) (Luo et al., 2022a) (Pine line indicates RTS number changes in the Honglianghe region (modified from Luo et al., 2022a), and blue histogram indicates thermokarst lake number changes on the central QTP (modified from Luo et al., 2022b), and (f–g) spatiotemporal variations in snow depth during 1980–2022 (Che et al., 2019; Yue et al., 2022).

changes the subglacial drainage channel. Thus, thermal control alters surging conditions and hydrological control triggers the surge (Peng et al., 2021; Zhang et al., 2022).

2.1.2. The 2016 Aru glacier collapse, western Qinghai–Tibet Plateau

Two glaciers, Aru Glacier No. 53 (Aru53) and Aru Glacier No. 50 (Aru50) in western Tibet, collapsed on 17 July, and 21 September 2016, respectively. Their deposit volumes were up to $(68 \pm 2) \times 10^6$ and $(83 \pm 2) \times 10^6$ m³. Aru53 ice avalanche

fan was 5.3 km long, 2.4 km wide, with an area of 9.4 km² and an average thickness of 7.5 m; Aru50 was 4.7 km long, 1.9 km wide, with an area of 6.5 km² and an average thickness of 30 m (Hu, 2018). Further glacial change analysis showed that the glacier area in Aru region decreased by $(0.4 \pm 4.1)\%$ from 1971 to 2016 with a negative mass balance of 0.15 ± 0.30 m w.e. per year in 1971–1999 and a positive mass balance of 0.33 ± 0.61 m per year in 1999–2016 (Zhang et al., 2018).

The huge ice body of Aru53 bursted into Lake Aru Co with tsunami-like waves and caused devastating destruction for

nearby environment, which was rare in the glacier collapse history. The ice collapse buried nine people, two vehicles and other living materials. Two months later, the main ice body of another glacier (Aru50) on the south side of Aru53 also collapsed. The surge-like behavior, climate driven glacier surface steepening, polythermal glacier structure, their geometry and slope, and liquid water from melt and rain during summer 2016 are considered to be the factors inducing this event (Kääb et al., 2018). Climate change is likely to be the main cause of these two extraordinary and unprecedented forms of glacier collapse. As the local temperature rises and precipitation increases, it may just be the beginning of a series of ice avalanche disaster in the future.

2.1.3. The 2022 glacier avalanche in central Tianshan, Kyrgyzstan

On 8 July, 2022 a group of hikers recorded a video of the Tianshan glacier collapse at Juuku Pass, Issyk-Kul, Kyrgyzstan, and two of them were slightly injured. The collapsed glacier is numbered G077865E41949N, with an area of 0.9 km². Its highest and lowest elevation are 4523 m and 4286 m, respectively (RGI, 2017). The glacier is affected by a westerly circulation and local airflow at Issyk-Kul. According to the measurements at Tianshan Mountain station (41.92°N, 78.23°E, 3614 m a.s.l.), which is nearest to this glacier, the annual precipitation is 200–500 mm.

In this event, the ice body collapsed at an altitude of 4330 m a.s.l., and the deposition area was at 3600 m a.s.l., with a horizontal distance of about 2 km. The analysis results of remote sensing data from SPOT7 showed that the glacier collapsed an area of 0.04 km² near the glacier termini (roughly 1/25 of the total glacier volume) and a sedimentary area of 0.52 km² has been formed. The average thickness of the deposition area is about 1.56 m, and the ice volume is about 0.82×10^6 m³. Furthermore, The planet remote sensing image on 8 July also showed that a large space in the deposition area was damaged. Ice temperature increase was considered as the main cause of the incident.

2.1.4. Recent icefall disconnection of Hailuogou Glacier, Mt. Gongga

The Hailuogou glacier is a temperate valley glacier under monsoon climate located in the southeastern Tibet. Although episode with a relative stable or slightly positive mass balance in 1980s during the dominated Little Ice Age retreat, the glacier has experienced accelerated shrinkage thereafter since 1990s (Liu et al., 2010). Its upper accumulation basin and the lower debris-covered ice tongue, connected by a 1080 m height ice fall, has dynamically disconnected since 2013 (Fig. 1). Losing the direct ice-flux transport, the lower ice tongue of Hailuogou glacier now is turning into a separate regenerated glacier, which will receive its accumulation from the collapsing ablation from the ‘new’ glacier above. Warming-induced rising equilibrium line altitude will lead to the accumulation-ablation ratio of upper glacier abruptly decreasing since a very large area of the glacier is situated in a wide cirque basin. A foreseen negative mass balance of the

upper part therefore will thus also impact the ‘health’ of the lower regenerated glacier. The disconnection of the HLG glacier is likely irreversible in the future unless experiencing an extreme and prolonged cold climate. For instance, as a sightseeing hotspot, tourist witnessed strong ice–water fall at the disconnection cliff of Hailuogou Glacier on 18 August 2018 and 8 July, 2022. This type of disconnection of ice falling glacier is a clear signal of tipping point for its irreversible change (Fig. 2).

2.1.5. The 2021 Chamoli massive ice-rock avalanche, North Indian Himalaya

The snow–ice–rock avalanches induced catastrophe mass flow and cascading geohazards show an increasing frequency and magnitude across HMA during the past decades, likely related to observed atmospheric warming and corresponding long-term changes in cryospheric conditions, e.g., glaciers shrinkage and permafrost thaw (McColl, et al., 2019). The 2021 catastrophic India Chamoli massive ice–rock avalanche is another case of hazardous tipping point happened on the high-altitude cryosphere (Shugar et al., 2021). Warming has increased the water phase changes in the upper mountain slopes and destabilized both the ice and its adjacent rock walls, causing an increased number and much larger magnitude, and even in low angle slopes, of hazardous ice–snow–rock collapse events in high mountain regions (Kääb, et al., 2021). Massive ice–rock collapse or ice–snow–rock avalanche mass flow can cause noticeable disasters since they potentially initiate catastrophic chain processes character by high mobility and long-run distance in the glacialized mountains. An increasing planned hydroelectric power projects, infrastructures, and human habitat communities must account for this tipping point of qualitative physical condition changes in high altitude ice–snow–rock environments.

2.1.6. The 2018–2021 glacial debris flow blockage in the Sedongpu basin, Yarlung Zangbo River

On 17 October 2018, a glacial debris flow/rock fall caused by ice avalanches occurred in the Sedongpu basin of Yarlung Zangbo River, near the village of Jiala, Linzhi city. It blocked the river and drowned several villages multiple times, and emergency management measures were carried out immediately to control the barrier lake. From remote sensing data, we find that the scale of this blockage incident was unusually large in history. The glaciers in Sedongpu basin are mostly monsoonal temperate glaciers and characterized by presence of debris in the ablation zones. All 12 glaciers in Sedongpu basin have retreated a lot since 1996, as seen from the Landsat and Sentinel-2A images. The average area reduction rates of these glaciers ranged from 0.26% to 8.29% during the periods of 1996–2004, 2004–2015 and 2015–2018, respectively. Overall, the total glacial area of the basin decreased by 9.65 km² (22.67%) from 1996 to 2018. The glacier shrinkage and glacier instability dynamics occurring in this region associated with the Yarlung Zangbo River are remarkable and have attracted intense attention because these rivers are



Fig. 2. Thinning, retreat and icefall disconnection of Hailuogou glacier (The picture in 1930 was taken by Arnold Heim. The, 2008–2022 pictures by Qiao Liu).

important freshwater resources for a large population not only on the Qinghai–Tibet Plateau but also in South Asia (Liu et al., 2014).

Following studies showed that Sedongpu basin continued to experience several river blocking events after this large-scale disasters (An et al., 2022). For example, up to four river blocking events induced by debris flow in Sedongpu basin during 2018–2019 (Tong et al., 2018; Liu et al., 2019). On 11 September 2019, a small-scale glacial debris flow in Sedongpu basin was detected. On 22 March 2021, Yarlung Zangbo River was once again blocked by a glacier/snow avalanche in Sedongpu basin (An et al., 2022). These river blocking disasters in Sedongpu basin were not rare incidents, and will continue to occur with increasing frequency under regional climate change. The glacier disasters in this region have arisen great risks to local socioeconomics under climate warming. Based on the ice avalanche frequency of the occurrence, it is identified that the Namjagbrawa Peak was one of the most dangerous places in HMA. In addition, these glacier hazards typically occurred between May and September, coinciding with the period of intense ablation of monsoonal temperate glaciers.

2.2. Increasing thermokarst activities in HMA

As a result of climate warming, the permafrost developed in HMA has degraded significantly since the 2000s (Zhao et al., 2021). The formation of thermokarst landscapes is an indicator of permafrost degradation and occurs mostly in ice-rich permafrost areas (Nitze et al., 2018; Ma et al., 2019; Luo et al., 2020; Serban et al., 2020). Thermokarst landforms, the most widespread forms of abrupt permafrost thaw, are widely distributed on the entire Qinghai–Tibet Plateau permafrost areas (Fig. 1d). Using high-resolution orthographic satellite images, Luo et al. (2022a) found that a total of 2669 active retrogressive thaw slump (RTS) were distributed on the entire Qinghai–Tibet Plateau. The average surface area of these RTSs is 1.44 hm², and the maximum density in a 25 km²

cell reaches 68 RTSs, which is higher than that reported in most of the previous studies in the Arctic and Subarctic (Nitze et al., 2018; Rudy et al., 2017; Segal et al., 2016). Wei et al. (2021) revealed that a total of ~161,300 thermokarst lakes ranging from 0.5 to 3 km² occurred over the Qinghai–Tibet Plateau, with a total area of $\sim 2825.45 \pm 5.75$ km². These lakes were unevenly distributed and mainly located in the Qiangtang basin, Yangtze River basin, and Yellow River basin.

Thermokarst activities in HMA have increased rapidly in recent decades, including the occurrence of thermokarst lakes and RTS. For example, combined with the historical aerial photographs and satellite images, Luo et al. (2022b) found that the number of RTSs significantly increased during 2008–2021 (Fig. 1e), which was closely related to high temperatures during the thawing season. Despite the rate of permafrost warming is only -0.2 °C per decade, a significant expansion of RTS has been observed along the Qinghai–Tibet Highway and in the Qilian Mountains regions of the HMA over the past few decades. Time-series monitoring of a RTS at K3035 mileage along the Qinghai–Tibet Highway revealed that the permafrost table was deepening in RTS development area, and that the affected area was gradually expanded (Niu et al., 2012). The number of RTS and the area affected by RTS in the Beilu River regions along the Qinghai–Tibet Highway have increased by 253% and 617% respectively from 2017 to 2018, posing a significant threat to engineering infrastructure stability (Luo et al., 2019). Time-series monitoring of the Qilian Mountains revealed a rapidly increasing trend in the rate of area growth and headwall retreat of RTS (Mu et al., 2020).

Luo et al. (2022b) found that a net increase in the thermokarst lake number of 4655 from 1969 to 2019 on the central Qinghai–Tibet Plateau (Fig. 1e), with the persistent climate warming and the increasing of precipitation were the most likely explanations for the observed results. There are about 250 thermokarst lakes distributed between the Fenghuo Mountain Pass and Kunlun Mountain Pass along the Qinghai–Tibet Railway, with a total area of about 1.39×10^6 m²,

causing great disturbance to the surrounding permafrost (Niu et al., 2011). Monitoring of thermokarst lakes in the Beilu River regions has shown continued expansion, resulting in the thawing of permafrost below the centre of the thermokarst lake and significant warming of the permafrost around the thermokarst lake (Lin et al., 2010). Permafrost meltwater and surface-subsurface inflow are vital to the water recharge and water balance of thermokarst lakes along the Qinghai–Tibet Highway, with surface precipitation accounting for only 14%–18% of the inflow to thermokarst lakes (Gao et al., 2018). In addition, permafrost degradation and the expansion of thermokarst landscapes have significantly increased sediment loads downstream since 1990s releasing organic carbon and nutrients that further affect local ecosystems (Zhang et al., 2022). The rapid development of thermokarst landscapes in the permafrost area of HMA will further accelerate permafrost degradation and organic carbon release, resulting in positive climate feedbacks and accelerated climate warming.

2.3. Snow depth anomaly in 2021/2022 winter

Snow cover is an important indicator of climate change over HMA. During 1980–2022, the average, maximum, and minimum snow depth exhibited a decrease (Fig. 1f). Spatially, the variations in snow depth displayed distinct patterns. Decreases were observed in the southeastern region, whereas increases were observed in the northern part and higher elevated areas (e.g., the Pamir Mountains). Notably, interannual variations in snow depth were evident, as it is influenced by both long-term climate change and short-term weather conditions.

We derived snow depth of the Qinghai–Tibet Plateau, main body of HMA, from passive microwave brightness temperature data by a modified Chang algorithm (Chang et al., 1987; Che et al., 2008) (Fig. 2). The brightness temperatures obtained from three sensors (SMMR, SMM/I, and SMMI/S) were cross-calibrated before being used (Dai et al., 2015). The coefficients of modified algorithm were dynamically adjusted based on the seasonal variation of grain size and snow density, and the influences from vegetation, wet snow, precipitation, cold desert, and frozen ground were removed. The snow depth dataset was validated using meteorological observation data, showing that the standard deviation is 6 cm.

Based on the dataset, we analyzed the daily snow depth in HMA over the last 31 years (1990–2001) and found that snow depth variations in some hydrological years showed a different pattern than in most years (Fig. 3). For example, the snow accumulation period was advanced in 1997/1998 and snow depth in the winter of 1997/1998 reached the maximum in during 1990–2021 period. Another example is that the snow depth in 2021/2022 had a similar variation pattern to 1997/1998 during the accumulation period, but the snow melt date in the spring of 2022 was significantly earlier than that of 1998 and other years. In the context of increasing extreme weather and climate events around the world (IPCC, 2021), we have to relate these abnormal states of snow cover variabilities to the

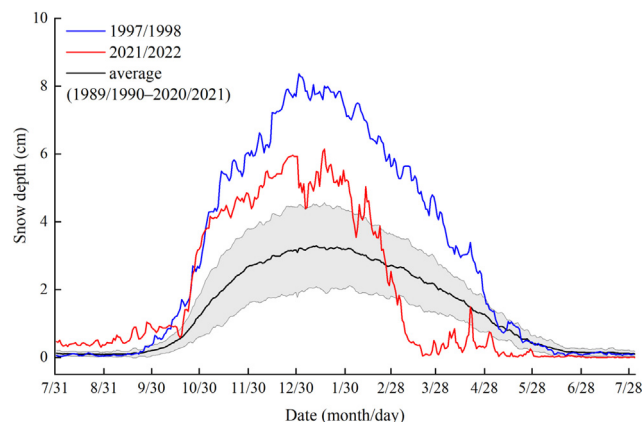


Fig. 3. Annual average pattern and abnormal pattern of daily snow depth in Qinghai–Tibet Plateau. (Data source: <https://www.tpdc.ac.cn/zh-hans/data/df40346a-0202-4ed2-bb07-b65dfcda9368>).

occurrence of China's 1998 floods and the 2022 drought in the Yangtze River basin.

Snow cover is not only a sensitive indicator that responds to the climate system, but is also an important feedback variable. Those changes in snow cover will in turn affect Earth's climate system via the surface energy budget, and influence freshwater resources across a large proportion of the Northern Hemisphere (Flanner et al., 2011; Immerzeel et al., 2010; Dery et al., 2007). Therefore, as a crucial element of the cryosphere, its anomaly is most likely an indirect cause or result of the occurrence of some tipping elements, as well as an important component of the new normal of nature formed after tipping elements. Therefore, we cannot ignore the importance and further investigation of snow cover.

3. Climate background of HMA that triggered ACEs

The HMA is recognized as a site of amplified global warming and a harbinger of global climate temperatures, showing heterogeneously rising temperatures over the past five decades (1971–2022). In the past five decades (1971–2022), the warming trends in HMA, which has expanded to the higher latitude regions, have exceeded the Asia regional and global mean value. Temperature increase throughout the HMA accelerated by 0.3 °C per decade during 1971–2022, almost doubling the global average (IPCC, 2021). Temperature change throughout the HMA is asymmetric, as the daily minimum temperature variation is much greater than the maximum temperature (Fig. 4).

The precipitation trends of HMA show a clear regional heterogeneity, increasing in the north and decreasing in the south, with positive trends over most of the central and eastern Himalaya and negative anomalies over the Karakoram, western Himalaya, and far eastern Himalaya. The westerly monsoon interactions result in precipitation variations at different altitudes throughout the HMA. This is also indicated by Fig. 5 where we can clearly see that the mean temperature anomaly in 2022 shows anomalous warming over a majority

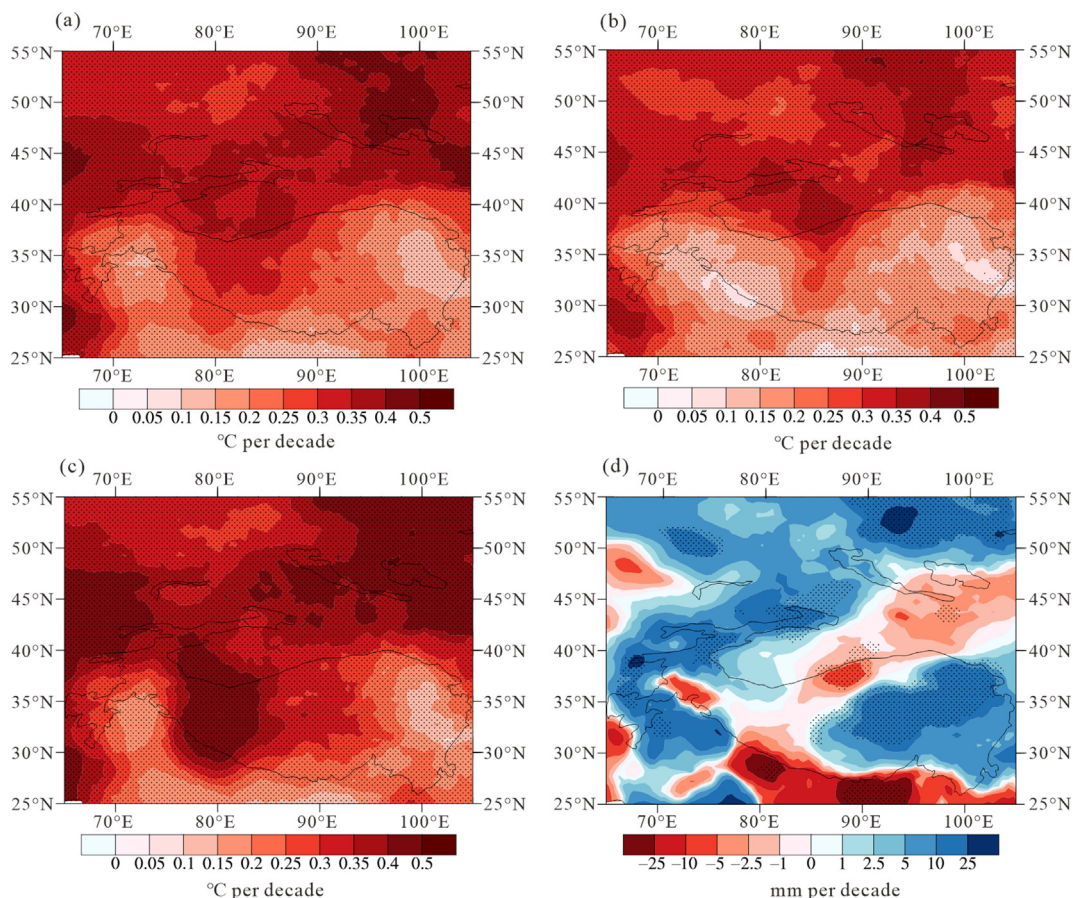


Fig. 4. Distribution of the trends of mean annual surface air temperature (a), maximum (b) and minimum air temperature (c) and precipitation (d) in the High Mountain Asia region for 1971–2022 (The area indicated by black contours is 2000 m a.s.l. Data source: CRU gridded dataset).

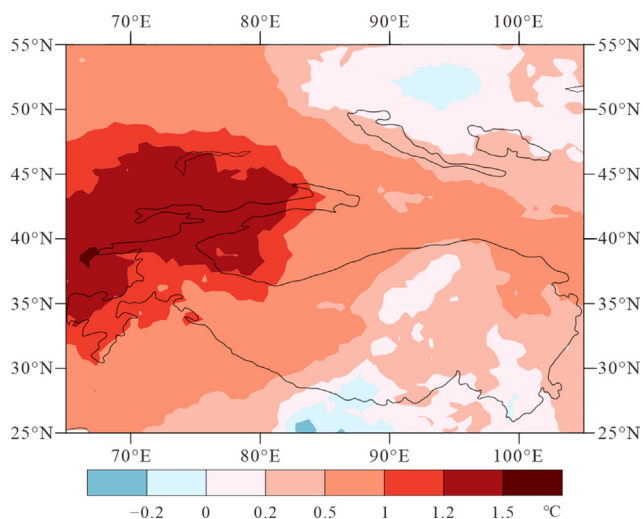


Fig. 5. Surface air temperature anomaly in the High Mountain Asia region relative to the 1991–2020 average for 2022 (The area indicated by black contours is 2000 m a.s.l. Data source: CRU gridded dataset).

region of HMA. The surface air temperatures of 2022 in most of the HMA region were remarkably higher than normal (average of 1991–2020), with the anomalies exceeding $+1.2\text{ °C}$ in the Kunlun mountains, Pamir mountains, Tianshan mountains and the northwestern Qinghai–Tibet Plateau. It can partly explain the rapid decrease of snow cover area as presented in Fig. 3.

4. Basic physical conditions of tipping points

4.1. Mountain glaciers

The dynamics of mountain glaciers are driven by gravity, and controlled by several ice flow mechanisms, i.e., internal deformation, basal slip, lateral drag and longitudinal stress gradient (Fig. 5a; Cuffey and Paterson, 2010). As climate gets warmer, the ice flow accelerates as higher temperature leads to softer ice and increases ice deformation. Meltwater will also lubricate glacier base and speed-up the ice flow, i.e., glacier dynamics may change abruptly in the existence of meltwater.

On one hand, the enhanced melt on the ice surface in the ablation region will penetrate into ice crevasses and release refreezing heat, which may possibly cause significant rise in englacial temperature. On the other hand, meltwater can reach glacier base and develop the subglacial hydrological system that imposes significant impacts on ice flow. A fully developed subglacial hydrology system can transport water from ice base outside of the glacier. However, at the early age of subglacial hydrological system development, the subglacial water pressure may increase and as a result, decrease the effective water pressure of the glacier and accelerate basal slip.

Traditionally, glacier models assume ice follows a power-law rheology, i.e., Glen's flow law, following a continuum mechanics theory. However, as stress exceeds some threshold value, failures may occur and a different constitutive law may apply. In this case, glacier ice tends to change towards a discrete flow pattern as ice becomes temperate and internal stress regime changes abruptly. When ice reaches the yield strength τ_y , the effective stress will not increase as ice stretches with an increasing strain rate ϵ_e , i.e., a decreasing ice viscosity μ ,

$$\mu = \frac{\tau_y}{2\epsilon_e} \quad (1)$$

This is following a 'plastic' failure rheology. Further, once ice reaches the failure threshold, the effective stress may also

decrease with increasing strain rate (Fig. 6b). Following Bassis et al. (2021) we can assume that the yield strength of ice decreases linearly with the strain accumulated in the yielded region (Eq. 2), which is a positive feedback mechanism that will enhance the ice failure (Bassiss et al., 2021) (see Fig. 7).

$$\tau_y = \max \left\{ \tau_c - (\tau_c - \tau_{\min}) \frac{\epsilon_p}{\epsilon_{\text{crit}}}, \tau_{\min} \right\} \quad (2)$$

where τ_c is the intact strength, τ_{\min} is a minimum yield strength after ice failure occurs and ϵ_{crit} is the strain rate value when ice failure happens.'

In addition to the changes of ice material, the basal slip condition may also contribute to an ice avalanche event. An ice-stream and shelf-like (free slip) at the bottom of glacier and a relatively large ice slope may get ice unbalanced and finally leads ice to collapse.

4.2. Permafrost

The rising air temperature and precipitation have increased the likelihood of slope movement and failure in alpine regions (Gariano and Guzzetti, 2016; Patton et al., 2019). Moreover, extreme warming and precipitation events promote active layer deepening and thawing of top-of-permafrost ice, which result in the increase of liquid water in the active layer and thus the pore water pressure (Lewkowicz and Way, 2019).

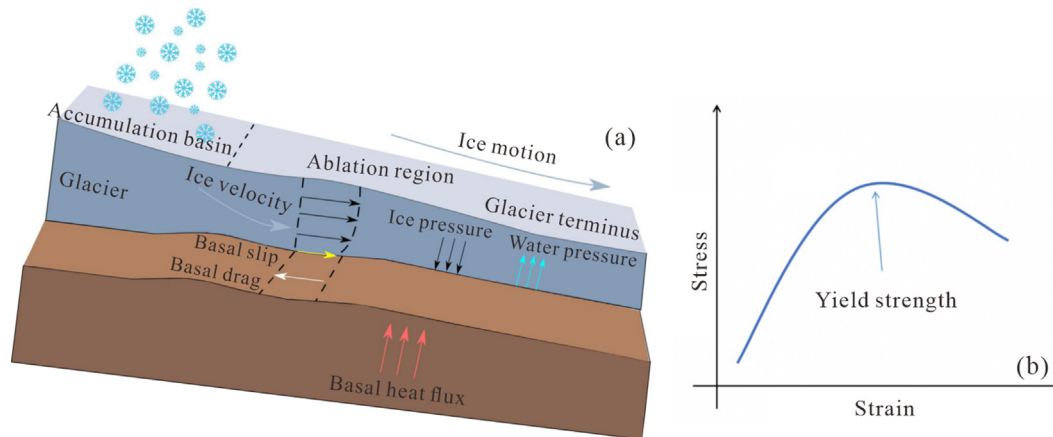


Fig. 6. A schematic of glacier ice flow and force balance (a), and (b) the yield strength of ice indicating a 'tipping point' of the relationship between the stress and strain of ice flow.

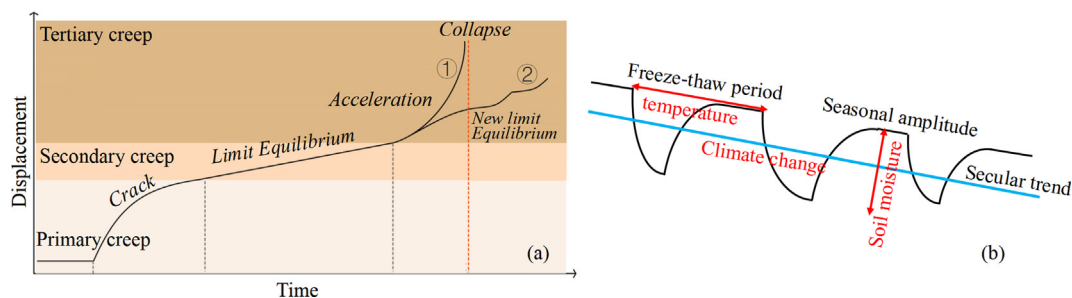


Fig. 7. Schematics of (a) three stages of kinematics-based failure mechanisms for slope instability: primary creep, secondary creep, and tertiary creep as indicated by different shading colors, and (b) the temporal evolution of ground deformation in permafrost environment (Hao et al., 2019) (A freeze-thaw period denotes one year between the current and the following thaw onset).

These processes may likely increase landslide activity (Huggel et al., 2012). In addition, the transition from frozen to unfrozen may dramatically reduce soil cohesion and unevenly shear strength especially in ice-rich permafrost environment, which aggravate abrupt permafrost thawing and landslide activity (Krautblatter et al., 2013; Fischer et al., 2013).

Generally, without considering pore pressure variations due to thaw consolidation, the slope stability factor of safety equation can be derived using the infinite slope model and the effective stress ultimate balance theory (Niu et al., 2005) and hydrothermal coupling model (Harlan et al., 1973). This type of model can be applied to estimate the dynamic instability of permafrost in HMA.

The failure of thaw slumps can be generally separated to three stages (Fig. 6a) (Hao et al., 2019). 1) In the first stage, primary creep occurs along an unstable surface under gravity, where uneven ground deformation and freeze–thaw processes may cause the formation of cracks. The ground exhibited a motion state along the slope by gravity; 2) the period of secondary stage is characterized by steady-state motion with a constant strain rate and limited equilibrium. Ground deformation is heterogeneous when the extrusion force or the friction coefficient becomes larger gradually; 3) after a period of relative stability, with the triggering events, such as extreme rainfall and thawing of topmost permafrost, an acceleration of ground movement may occur and eventually lead to slope collapse. The ground deformation in permafrost regions can be generally represented by a long-term subsidence trend and a seasonal component (Fig. 6b). The subsidence trends are mainly related to the thawing of topmost permafrost and the downslope creeping, whereas the seasonal deformation originates from the soil volumetric changes due to water-ice phase transition.

5. Final remarks

The cryosphere is considered as an amplification of climate change, especially the Arctic, west Antarctica, and the Qinghai–Tibet Plateau (Xiao et al., 2015; Qin et al., 2018). Under global warming, the increase in air temperature at high-elevation areas is noticeably greater than the global mean (An et al., 2017), accompanied with shrinking glaciers and intensified glacial activities all over the world (Pritchard, 2019; Milillo et al., 2019; Maurer et al., 2019). Agriculture, living stocks, infrastructure, cities and oasis, pasture lands over HMA is highly depending on cryospheric services (Xiao et al., 2015; Su et al., 2021), but at the same time, they are also under potential threats of abrupt events as above.

When the regional warming rate rises to the extreme level of triggering abrupt events, these events will exert large damages to local socioeconomics. For instance, according to the statistics from local governments, surge and ice avalanche of Karayaylak Glacier in 2015 had corroded 60.7 km² of grassland and resulted in the disappearance of more than 100 livestock. Glacial debris flow blockage in the Sedongpu basin has caused severe damages to local lives, providing a strong evidence that glacial debris flow is the dominant hazard in

those regions. Glacier collapsed at Juuku Pass of Kyrgyzstan injured two people among a group of hikers. However, ice fall at Heiluogou Glacier is far from tourist, the frequent events in summer might be an attraction hotspot for sightseeing.

In summary, from the observations at present and during the past several decades, it is clear that the glacier, snow cover and permafrost in HMA is approaching to the tipping points. Some of the events may have even passed the tipping points (e.g., glacier avalanches). Thus, we suggest the earlier warning system should be established by studying high risk areas of ACEs. The system should contain hazards (ACEs), vulnerability, as well as exposure of socioeconomic aspects. Upon the fully consideration on geological and climatic conditions, more attentions should be paid to large glaciers, for moraines and water storage (mainly glacial lake) are carriers of destructive force. Usually, short-term heavy rainfall is regarded as a triggering factor for landslides and debris flows and has been considered in almost all researches/early warning schemes, because it brings massive melting in glaciers and rising in glacial lakes, leading to debris flows, glacial lake outbursts, etc. We suggest to consider earthquake as an important factor of glacier hazards/disasters, for it can rupture the internal glacier structure from a large distance and trigger a collapse a few months later. In addition, environmental protection, such as afforestation, construction of infrastructure in non-disaster-prone areas and strengthening local people's awareness of disaster prevention are invaluable.

Credit author statement

Zhi-Qiang Wei: Formal analysis, Methodology. Dong-Hui Shangguan: Formal analysis, Methodology. Fei-Teng Wang: Formal analysis, Methodology. Qiao Liu: Formal analysis, Methodology. Chun-Hai Xu: Validation, Visualization. Cun-De Xiao: Writing – original draft, Conceptualization, Writing – review & editing. Xin-Wu Xu: Validation, Visualization. Tong Zhang: Formal analysis, Methodology, Writing – review & editing. Peng-Ling Wang: Formal analysis, Methodology. Jie Chen: Visualization, Validation. Tao Che: Formal analysis, Methodology. Ming-Hu Ding: Formal analysis, Methodology. Da-He Qin: Writing – review & editing, Supervision. Tong-Hua Wu: Formal analysis, Methodology. Lei Huang: Methodology, Formal analysis.

Declaration of competing interest

The authors declare no conflict of interest.

Acknowledgment

This work was supported by the National Key Research and Development Program of China (2022YFF0801903), the National Natural Science Foundation of China (41690145, 42125604), the State Key Laboratory of Earth Surface Processes and Resource Ecology (2021-TS-06, 2021-KF-06, and 2022-ZD-05), the Fundamental Research Funds for the Central Universities (2021NTST16), the Beijing Normal University

Talent Introduction Project of China (12807–312232101), and Basic Research Fund of CAMS (2023Z004). Yuzhe Wang, Yi Huang and Hongyu Zhao also contributed to the figure improvements. We thank two anonymous reviewers for their improvements of the manuscript.

References

- An, B., Wang, W., Yang, W., et al., 2022. Process, mechanisms, and early warning of glacier collapse-induced river blocking disasters in the Yarlung Tsangpo Grand Canyon, southeastern Tibetan Plateau. *Sci. Total Environ.* 816, 151652. <https://doi.org/10.1016/j.scitotenv.2021.151652>.
- An, W., Hou, S., Hu, Y., et al., 2017. Delayed warming hiatus over the Tibetan Plateau. *Earth Space Sci.* 4, 128–137. <https://doi.org/10.1002/2016EA000179>.
- Acharya, A., Steiner, J.F., Walizada, K.M., et al., 2023. Snow and ice avalanches in High Mountain Asia: scientific, local and indigenous knowledge. *Nat. Hazards Earth Syst. Sci.* 23, 2569–2592. <https://doi.org/10.5194/nhess-23-2569-2023>.
- Bassis, J.N., Berg, B., Crawford, A.J., et al., 2021. Transition to marine ice cliff instability controlled by ice thickness gradients and velocity. *Science* 372 (6548), 1342–1344. <https://doi.org/10.1126/science.abf627>.
- Brun, F., Berthier, E., Wagnon, P., et al., 2017. A spatially resolved estimate of High Mountain Asia glacier mass balances from 2000 to 2016. *Nat. Geosci.* 10, 668–673. <https://doi.org/10.1038/ngeo2999>.
- Chang, A.T.C., Foster, J.L., Hall, D.K., 1987. Nimbus-7 SMMR derived GlobSnow snow cover parameters. *Ann. Glaciol.* 9, 39–44. <https://doi.org/10.3189/S0260305500200736>.
- Che, T., Li, X., Jin, R., et al., 2008. Snow depth derived from passive microwave remote-sensing data in China. *Ann. Glaciol.* 49, 145–154. <https://doi.org/10.3189/172756408787814690>.
- Che, T., Hao, X., Dai, L., et al., 2019. Snow cover variation and its impacts over the Qinghai–Tibet Plateau. *Bull. Chin. Acad. Sci.* 34 (11), 5. <https://doi.org/10.16418/j.issn.1000-3045.2019.11.007> (Chinese).
- Chen, D., Xu, B., Yao, T., et al., 2015. Assessment of environmental change of the Tibetan Plateau, past, present and future. *Sci. Bull.* 60, 3025–3035. <https://doi.org/10.1360/N972014-01370> (Chinese).
- Cuffey, K.M., Paterson, W.S.B., 2010. *The Physics of Glaciers*, fourth ed. Butterworth-Heinemann, Oxford.
- Dai, L., Che, T., Ding, Y., 2015. Inter-calibrating SMMR, SSM/I and SSM/I/S data to improve the consistency of snow-depth products in China. *Rem. Sens.* 7, 7212–7230. <https://doi.org/10.3390/rs70607212>.
- Déry, S.J., Brown, R.D., 2007. Recent Northern Hemisphere snow cover extent trends and implications for the snow-albedo feedback. *Geophys. Res. Lett.* 34, 2–7. <https://doi.org/10.1029/2007gl031474>.
- Fischer, L., Huggel, C., Kääb, A., et al., 2013. Slope failures and erosion rates on a glacierized high-mountain face under climatic changes. *Earth Surf. Process. Landforms* 38 (8), 836–846. <https://doi.org/10.1002/esp.3355>.
- Flanner, M.G., Shell, K.M., Barlage, M., et al., 2011. Radiative forcing and albedo feedback from the Northern Hemisphere cryosphere between 1979 and 2008. *Nat. Geosci.* 4, 151–155. <https://doi.org/10.1038/ngeo1062>.
- Gao, Z., Niu, F., Lin, Z., et al., 2018. Evaluation of thermokarst lake water balance in the Qinghai–Tibet Plateau via isotope tracers. *Sci. Total Environ.* 636, 1–11. <https://doi.org/10.1016/j.scitotenv.2018.04.103>.
- Gariano, S.L., Guzzetti, F., 2016. Landslides in a changing climate. *Earth Sci. Rev.* 162, 227–252. <https://doi.org/10.1016/j.earscirev.2016.08.011>.
- Gilbert, A., Leinss, S., Kargel, J., et al., 2018. Mechanisms leading to the 2016 giant twin glacier collapses, Aru Range, Tibet. *Cryosphere* 12, 2883–2900. <https://doi.org/10.5194/tc-12-2883-2018>.
- Hao, J., Wu, T., Wu, X., et al., 2019. Investigation of a small landslide in the Qinghai–Tibet Plateau by InSAR and absolute deformation model. *Rem. Sens.* 11 (18), 2126. <https://doi.org/10.3390/rs11182126>.
- Harlan, R.L., 1973. Analysis of coupled heat-fluid transport in partially frozen soil. *Water Resour. Res.* 9 (5), 1314–1323. <https://doi.org/10.1029/WR009i005p01314>.
- Hu, W., Yao, T., Yu, W., et al., 2018. Advances in the study of glacier avalanches in High Asia. *J. Glaciol. Geocryol.* 40 (6), 1141–1152. <https://doi.org/10.7522/j.issn.1000-0240.2018.0504> (Chinese).
- Huggel, C., Clague, J.J., Korup, O., 2012. Is climate change responsible for changing landslide activity in high mountains? *Earth Surf. Process. Landforms* 37 (1), 77–91. <https://doi.org/10.1002/esp.2223>.
- Immerzeel, W.W., van Beek, L.P.H., Bierkens, M.F.P., 2010. Climate change will affect the Asian water towers. *Science* 328, 1382–1385. <https://doi.org/10.1126/science.1183188>.
- IPCC, 2021. *Climate Change 2021: The Physical Science Basis. Contribution of Working Group I to the Sixth Assessment Report of the Intergovernmental Panel on Climate Change*. Cambridge University Press, Cambridge and New York.
- Kääb, A., Jacquemart, M., Gilbert, A., et al., 2021. Sudden large-volume detachments of low-angle mountain glaciers: more frequent than thought? *Cryosphere* 15 (4), 1751–1785. <https://doi.org/10.5194/tc-15-1751-2021>.
- Krautblatter, M., Funk, D., Günzel, F.K., 2013. Why permafrost rocks become unstable: a rock–ice mechanical model in time and space. *Earth Surf. Process. Landforms* 38 (8), 876–887. <https://doi.org/10.1002/esp.3374>.
- Kääb, A., Leinss, S., Gilbert, A., et al., 2018. Massive collapse of two glaciers in western Tibet in 2016 after surge-like instability. *Nat. Geosci.* 11, 114–120. <https://doi.org/10.1038/s41561-017-0039-7>.
- Lewkowicz, A.G., Way, R.G., 2019. Extremes of summer climate trigger thousands of thermokarst landslides in a High Arctic environment. *Nat. Commun.* 10, 1329. <https://doi.org/10.1038/s41467-019-09314-7>.
- Li, Z., Chen, H., Miao, W., 2017. Research report on the mechanism of Karayaylak Glacier in Western Kunlun Mountains and glacier disaster in China–Pakistan Economic Corridor. Xinjiang Uygur Autonomous Region Development and Reform Commission, Urumqi.
- Lin, Z., Niu, F., Xu, Z., et al., 2010. Thermal regime of a thermokarst lake and its influence on permafrost, Beiluhe basin, Qinghai–Tibet Plateau. *Permafrost. Periglac. Process.* 21 (4), 315–324. <https://doi.org/10.1002/ppp.692>.
- Liu, C., Lü, J., Tong, L., et al., 2019. Research on glacial/rock fall-landslide-debris flows in Sedongpu basin along Yarlung Zangbo River in Tibet. *Chin. Geol.* 46 (2), 219–234. <https://doi.org/10.12029/gc20190201> (Chinese).
- Liu, W., Xu, Z., Li, F., et al., 2014. Climate change scenarios in the Yarlung Zangbo river basin based on the ASD model. *Plateau Meteorol.* 33 (1), 26–36. <https://doi.org/10.7522/j.issn.1000-0534.2012.00176> (Chinese).
- Liu, Q., Liu, S., Zhang, Y., et al., 2010. Recent shrinkage and hydrological response of Hailuoguo glacier, a monsoon temperate glacier on the east slope of Mount Gongga, China. *J. Glaciol.* 56 (196), 215–224. <https://doi.org/10.3189/002214310791968520>.
- Luo, D., Jin, H., Du, H., et al., 2020. Variation of alpine lakes from 1986 to 2019 in the headwater area of the Yellow River, Tibetan Plateau using google Earth engine. *Adv. Clim. Change Res.* 11 (1), 11–21. <https://doi.org/10.1016/j.accre.2020.05.007>.
- Luo, J., Niu, F., Lin, Z., et al., 2019. Recent acceleration of thaw slumping in permafrost terrain of Qinghai–Tibet Plateau: an example from the Beiluhe Region. *Geomorphology* 341, 79–85. <https://doi.org/10.1016/j.geomorph.2019.05.020>.
- Luo, J., Niu, F., Lin, Z., et al., 2022a. Inventory and frequency of retrogressive thaw slumps in permafrost region of the Qinghai–Tibet Plateau. *Geophys. Res. Lett.* 49 (23), e2022GL099829. <https://doi.org/10.1029/2022GL099829>.
- Luo, J., Niu, F., Lin, Z., et al., 2022b. Abrupt increase in thermokarst lakes on the central Tibetan Plateau over the last 50 years. *Catena* 217, 106497. <https://doi.org/10.1016/j.catena.2022.106497>.
- Ma, Q., Jin, H., Bense, V.F., et al., 2019. Impacts of degrading permafrost on streamflow in the source area of Yellow River on the Qinghai–Tibet Plateau, China. *Adv. Clim. Change Res.* 10 (4), 225–239. <https://doi.org/10.1016/j.accre.2020.02.001>.
- Maurer, J.M., Schaefer, J.M., Rupper, S., et al., 2019. Acceleration of ice loss across the Himalayas over the past 40 years. *Sci. Adv.* 5 (6), eaav7266. <https://doi.org/10.1126/sciadv.aav7266>.
- McColl, S.T., Draebing, D., 2019. Rock slope instability in the Proglacial Zone: state of the art, geomorphology of proglacial systems. In: Heckmann, T., Morche, D. (Eds.), *Geomorphology of Proglacial Systems. Geography of the Physical Environment*. pp. 119–141. Springer, Cham. https://doi.org/10.1007/978-3-319-94184-4_8.

- McKay, A., Staal, A., Abrams, J., et al., 2022. Exceeding 1.5°C global warming could trigger multiple climate tipping points. *Science* 377 (6611), 1171. <https://doi.org/10.1126/science.abn7950>.
- Milillo, P., Rignot, E., Rizzoli, P., et al., 2019. Heterogeneous retreat and ice melt of thwaites glacier, west Antarctica. *Sci. Adv.* 5 (1). <https://doi.org/10.1126/sciadv.aau3433> eaa03433.
- Mu, C., Shang, J., Zhang, T., et al., 2020. Acceleration of thaw slump during 1997–2017 in the qilian mountains of the northern Qinghai–Tibetan plateau. *Landslides* 17 (5), 1051–1062. <https://doi.org/10.1007/s10346-020-01344-3>.
- Nitze, I., Grosse, G., Jones, B.M., et al., 2018. Remote sensing quantifies widespread abundance of permafrost region disturbances across the Arctic and Subarctic. *Nat. Commun.* 9 (1), 1–11. <https://doi.org/10.1038/s41467-018-07663-3>.
- Niu, F., Cheng, G., Ni, W., et al., 2005. Engineering-related slope failure in permafrost regions of the Qinghai–Tibet Plateau. *Cold Reg. Sci. Technol.* 42 (3), 215–225. <https://doi.org/10.1016/j.coldregions.2005.02.002>.
- Niu, F., Lin, Z., Liu, H., et al., 2011. Characteristics of thermokarst lakes and their influence on permafrost in Qinghai–Tibet Plateau. *Geomorphology* 132 (3–4), 222–233. <https://doi.org/10.1016/j.geomorph.2011.05.011>.
- Niu, F., Luo, J., Lin, Z., et al., 2012. Development and thermal regime of a thaw slump in the Qinghai–Tibet Plateau. *Cold Reg. Sci. Technol.* 83, 131–138. <https://doi.org/10.1016/j.coldregions.2012.07.007>.
- Obu, J., Westermann, S., Bartsch, A., et al., 2019. Northern Hemisphere permafrost map based on TTOP modelling for 2000–2016 at 1 km² scale. *Earth Sci. Rev.* 193, 299–316. <https://doi.org/10.1016/j.earscirev.2019.04.023>.
- Patton, A.I., Rathburn, S.L., Capps, D.M., 2019. Landslide response to climate change in permafrost regions. *Geomorphology* 340, 116–128. <https://doi.org/10.1016/j.geomorph.2019.04.029>.
- Peng, Y., Li, Z., Xu, C., et al., 2021. Surface velocity analysis of surge region of karayaylak glacier from 2014 to 2020 in the pamir plateau. *Rem. Sens.* 13 (4), 774. <https://doi.org/10.3390/rs13040774>.
- Pfeffer, W.T., Arendt, A.A., Bliss, A., et al., 2014. The Randolph glacier inventory: a globally complete inventory of glaciers. *J. Glaciol.* 60 (221), 537–552. <https://doi.org/10.3189/2014JoG13J176>.
- Pritchard, H.D., 2019. Asia's shrinking glaciers protect large populations from drought stress. *Nature* 569, 649–654. <http://doi.org/s4158601912401>.
- Qin, D., Ding, Y., Xiao, C., et al., 2018. Cryospheric science: research framework and disciplinary system. *Natl. Sci. Rev.* 5, 255–268. <https://doi.org/10.1093/nsr/nwx108>.
- RGI (Randolph Glacier Inventory) Consortium, 2017. A Dataset of Global Glacier Outlines: Version 6.0. Technical Report, Global Land Ice Measurements from Space. Digital Media, Colorado, USA. <https://doi.org/10.7265/N5-RGI-60>.
- Rudy, A.C.A., Lamoureux, S.F., Kokelj, S.V., et al., 2017. Accelerating thermokarst transforms ice-cored terrain triggering a downstream cascade to the ocean. *Geophys. Res. Lett.* 44 (21), 11080–11087. <https://doi.org/10.1002/2017GL074912>.
- Segal, R.A., Lantz, T.C., Kokelj, S.V., 2016. Acceleration of thaw slump activity in glaciated landscapes of the Western Canadian Arctic. *Environ. Res. Lett.* 11, 034025. <https://doi.org/10.1088/1748-9326/11/3/034025>.
- Serban, D.R., Jin, H., Serban, M., et al., 2020. Mapping thermokarst lakes/ponds across permafrost landscapes in the headwater area of Yellow River on NE Qinghai–Tibet Plateau. *Int. J. Rem. Sens.* 41 (18), 7042–7067. <https://doi.org/10.1080/01431161.2020.1752954>.
- Shangguan, D., Liu, S., Ding, Y., et al., 2016. Characterizing the May 2015 Karayaylak Glacier surge in the eastern Pamir Plateau using remote sensing. *J. Glaciol.* 62 (235), 944–953. <https://doi.org/10.1017/jog.2016.81>.
- Shugar, D.H., Jacquemart, M., Shean, D., et al., 2021. A massive rock and ice avalanche caused the 2021 disaster at Chamoli, Indian Himalaya. *Science* 373 (6552), 300–306. <https://doi.org/10.1126/science.abh4455>.
- Su, B., Xiao, C., Chen, D., et al., 2021. Mismatch between the population and meltwater changes creates opportunities and risks for global glacier-fed basins. *Sci. Bull.* 67, 9–12. <https://doi.org/10.1016/j.scib.2021.07.027>.
- Tong, L., Tu, J., Pei, L., et al., 2018. Preliminary discussion of the frequently debris flow events in Sedongpu Basin at Gyalaperi peak, YarlungZangbo River. *J. Eng. Geol.* 26 (6), 1552–1561. <https://doi.org/10.13544/j.cnki-jeg.2018-401> (Chinese).
- Wei, Z., Du, Z., Wang, L., et al., 2021. Sentinel-based inventory of thermokarst lakes and ponds across permafrost landscapes on the Qinghai–Tibet Plateau. *Earth Space Sci.* 8 (11), e2021EA001950. <https://doi.org/10.1029/2021EA001950>.
- Xiao, C., Wang, S., Qin, D., 2015. A preliminary study of cryosphere service function and value evaluation. *Adv. Clim. Change Res.* 6 (3), 181–187. <https://doi.org/10.1016/j.accre.2015.11.004>.
- Yao, T., Xue, Y., Chen, D., et al., 2019. Recent third pole's rapid warming accompanies cryospheric melt and water cycle intensification and interactions between monsoon and environment: multidisciplinary approach with observations, modeling, and analysis. *Bull. Am. Meteorol. Soc.* 100, 423–444. <https://doi.org/10.1175/BAMS-D-17-0057.1>.
- Yue, S., Che, T., Dai, L., et al., 2022. Characteristics of snow depth and snow phenology in the high latitudes and high altitudes of the Northern Hemisphere from 1988 to 2018. *Rem. Sens.* 14, 5057. <https://doi.org/10.3390/rs14195057>.
- Zhang, T., Li, D., East, A.E., et al., 2022. Warming-driven erosion and sediment transport in cold regions. *Nat. Rev. Earth Environ.* 3, 832–851. <https://doi.org/10.1038/s43017-022-00362-0>.
- Zhang, Z., Liu, S., Zhang, Y., et al., 2018. Glacier variations at Aru Co in western Tibet from 1971 to 2016 derived from remote-sensing data. *J. Glaciol.* 64 (245), 397–406. <https://doi.org/10.1017/jog.2018.34>.
- Zhang, Z., Tao, P., Liu, S., et al., 2022. What controls the surging of Karayaylak glacier in eastern Pamir? New insights from remote sensing data. *J. Hydrol.* 607, 127577. <https://doi.org/10.1016/j.jhydrol.2022.127577>.
- Zhang, Y., Liu, Y., Su, P., et al., 2023. Advances in the study of glacier avalanches in Tibet. *Chin. J. Geol. Hazard Control* 34 (2), 132–145. <https://doi.org/10.16031/j.cnki.issn.1003-8035.202110022> (Chinese).
- Zhao, L., Zou, D., Hu, G., et al., 2021. A synthesis dataset of permafrost thermal state for the Qinghai–Tibet (Xizang) Plateau, China. *Earth Syst. Sci. Data* 13, 4207–4218. <https://doi.org/10.5194/essd-13-4207-2021>.